

Article

A Luminescent Terbium MOF Containing Hydroxyl Groups Exhibits Selective Sensing of Nitroaromatic Compounds and Fe(III) Ions

Sanchari Pal, and Parimal K. Bharadwaj

Cryst. Growth Des., **Just Accepted Manuscript** • DOI: 10.1021/acs.cgd.6b00930 • Publication Date (Web): 29 Aug 2016Downloaded from <http://pubs.acs.org> on August 31, 2016

Just Accepted

“Just Accepted” manuscripts have been peer-reviewed and accepted for publication. They are posted online prior to technical editing, formatting for publication and author proofing. The American Chemical Society provides “Just Accepted” as a free service to the research community to expedite the dissemination of scientific material as soon as possible after acceptance. “Just Accepted” manuscripts appear in full in PDF format accompanied by an HTML abstract. “Just Accepted” manuscripts have been fully peer reviewed, but should not be considered the official version of record. They are accessible to all readers and citable by the Digital Object Identifier (DOI®). “Just Accepted” is an optional service offered to authors. Therefore, the “Just Accepted” Web site may not include all articles that will be published in the journal. After a manuscript is technically edited and formatted, it will be removed from the “Just Accepted” Web site and published as an ASAP article. Note that technical editing may introduce minor changes to the manuscript text and/or graphics which could affect content, and all legal disclaimers and ethical guidelines that apply to the journal pertain. ACS cannot be held responsible for errors or consequences arising from the use of information contained in these “Just Accepted” manuscripts.



1
2
3
4
5
6
7
8
9

A Luminescent Terbium MOF Containing Hydroxyl Groups Exhibits Selective Sensing of Nitroaromatic Compounds and Fe(III) Ions

10 Sanchari Pal and Parimal K. Bharadwaj*

11 *Department of Chemistry, Indian Institute of technology Kanpur, 208016, India*

12 *Email: pkb@iitk.ac.in*

13
14
15
16
17
18
19 **ABSTRACT:** A new 3D porous Tb(III)-ion based PMOF,
20 $\{[\text{Tb}(\text{L})(\text{DMA})].(\text{DMA}).(0.5\text{H}_2\text{O})\}$ (1) (where $\text{L} = \text{L}^{3-}$, $\text{H}_3\text{L} = 3'$ -hydroxybiphenyl-3,4',5-
21 tricarboxylic acid) with uncoordinated hydroxyl groups decorating the pores have been
22 solvothermally synthesized in moderate yield. The hydroxyl groups act as potential interaction
23 sites to sensitize the luminescence output of the Tb^{3+} ion. Luminescence studies reveal that the
24 PMOF can selectively and reversibly sense nitroaromatic compounds and Fe(III) ions in DMF
25 suspension through fluorescence quenching observable under UV light. For the nitroaromatic
26 compounds, it is the host-guest interactions with the PMOF while for Fe^{3+} ion, it is the
27 competitive absorption of excitation energy that are the probable mechanisms for such sensing
28 processes.
29
30
31
32
33
34
35
36
37
38
39
40
41
42
43
44
45
46
47
48
49
50
51
52
53
54
55
56
57
58
59
60

INTRODUCTION

Design, synthesis and characterization of porous metal organic frameworks (PMOFs) continue to be a subject of intense research owing to their various practical applications.¹⁻⁷ Particularly, chemical sensing through change in the luminescence properties of PMOFs is of great practical importance.⁸⁻¹¹ The capability of host-guest interactions that modulate the luminescence output of PMOFs make them promising candidates as chemical sensors.

Sensing of nitroaromatic compounds (NACs) as well as cations especially Fe^{3+} ions are of practical significance. Nitroaromatic compounds pose serious environmental hazards due to their explosive nature.¹² For example, compounds such as nitrobenzene (NB), 4-nitrotoluene (NT), 2,4-dinitrotoluene (DNT), trinitrotoluene (TNT) and so on, are on the list of anti-terrorism or environment security in different countries. Trinitrophenol (TNP) is very toxic to human health and its usage in the chemical industry may lead to fatal environmental consequences. Metabolism of TNP generates picramic acid (2-amino-4,6-dinitrophenol) as a by-product that shows ten times more mutagenic activity than TNP.¹³ Due to moderate vapor pressure and limited chemical reactivity, detection of NACs is not easy. Although different analytical techniques are known to detect NACs, they are either very expensive and time-consuming, or are difficult to operate.¹⁴ However, NACs being electron-deficient compounds can possibly enter into the voids of a porous luminescent PMOF that provides electron-rich environment. The efficient host-guest interactions can modulate the luminescence characteristics of the PMOF thus providing a rapid, inexpensive technique for the detection of trace quantities of NACs. On the other hand, detection of Fe^{3+} is also very important since it is a vital element in the environment as well as in biological systems. It is best known for its role in hemoglobin formation, electron transfer, oxygen metabolism processes, in the synthesis of DNA and RNA, etc. Deviation from

normal permissible limit of iron concentration causes serious health disorders. Accumulated data on iron metabolism suggest that alterations in the intracellular pool of 'redox-active' iron (also called 'chelatable iron') can contribute substantially to a variety of injurious processes such as ischemia-reperfusion injury, ethanol toxicity and oxidative injury after nutrient deprivation and so on.¹⁵

Lanthanide containing PMOFs have drawn immense attention for their sensing applications.¹⁶ The emission from a lanthanide ion is generally weak because it involves spin- and/or parity-forbidden f-f transitions. Integration of these ions with π -conjugated organic linkers enables electron transfer upon excitation from the linker to the lanthanide ion that greatly enhances its characteristic emission. This phenomenon is known as the “antenna effect” (Figure 1).¹⁷ In lanthanide containing PMOFs, inclusion of guest molecules can alter the emission intensity by interrupting the electron transfer due to favorable host-guest interactions. Since the emission profiles of lanthanide ions are highly characteristic and can be easily observed under standard UV-lamp, it offers advantages over d^{10} metal ion based PMOF sensors though there are several reports of the d^{10} metal ion based PMOF showing high selectivity and sensitivity for the detection of NACs.¹⁸⁻²³ In recent years, a few $\text{Eu}^{3+}/\text{Tb}^{3+}$ based luminescent PMOFs have been reported for the detection of nitroaromatics²⁴⁻²⁷ and different metal ions.²⁸⁻³²

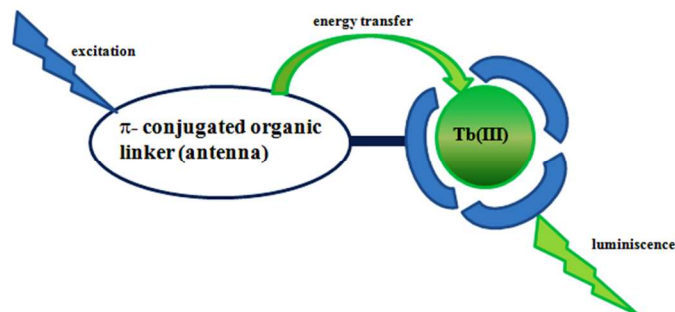


Figure 1. “Antenna effect” induced luminescence in **1**.

1
2
3 In the present work, a new rigid linear linker has been designed to provide uncoordinated
4 hydroxyl groups in the pores. It forms a 3D PMOF, $\{[\text{Tb}(\text{L})(\text{DMA})].(\text{DMA}).(0.5\text{H}_2\text{O})\}$ (1)
5
6 (where $\text{L}=\text{L}^{3-}$, $\text{H}_3\text{L}=3'$ -hydroxybiphenyl-3,4',5-tricarboxylic acid) with uncoordinated hydroxyl
7
8 groups decorating the channels and hosting highly disordered solvent molecules in the pore. It
9
10 emits bright visible characteristic green light under UV-lamp. The luminescence is selectively
11
12 quenched by nitroaromatic compounds and Fe^{3+} ions in DMF suspension.
13
14
15
16
17
18
19

20 EXPERIMENTAL SECTION

21 Materials and measurements

22
23 Reagent grade methyl-4-iodosalicylate, benzyl bromide, PdCl_2 , $\text{Tb}(\text{NO}_3)_3 \cdot 6\text{H}_2\text{O}$, were
24
25 procured from Sigma-Aldrich and used as received. All solvents were obtained from S. D. Fine
26
27 Chemicals, India and purified following established procedures prior to use. Characterizations of
28
29 the linker have been carried out by a number of spectroscopic techniques as detailed
30
31 previously.³³ Powder X-Ray diffraction (PXRD) patterns of the compounds were recorded with a
32
33 Bruker D8 Advance diffractometer equipped with nickel filtered CuK_α radiation.
34
35 Thermogravimetric analyses (TGA) (5 °C/min heating rate under nitrogen atmosphere) were
36
37 performed with a Mettler Toledo Star System. Solid-state as well as dispersed phase absorption
38
39 and emission spectra were recorded using UV–VIS–NIR spectrophotometer (Varian Model Cary
40
41 5000) and Jobin Yvon Horiba Fluorolog-3 spectrofluorimeter at room temperature. EDS analysis
42
43 was done using Tungsten-Electron-Microscope (JSM-6010LA; JEOL). Gas adsorption
44
45 measurements were performed using automatic volumetric BELSORP-MINI-II adsorption
46
47 equipment.
48
49
50
51
52
53
54
55
56
57
58
59
60

Single crystal X-ray studies

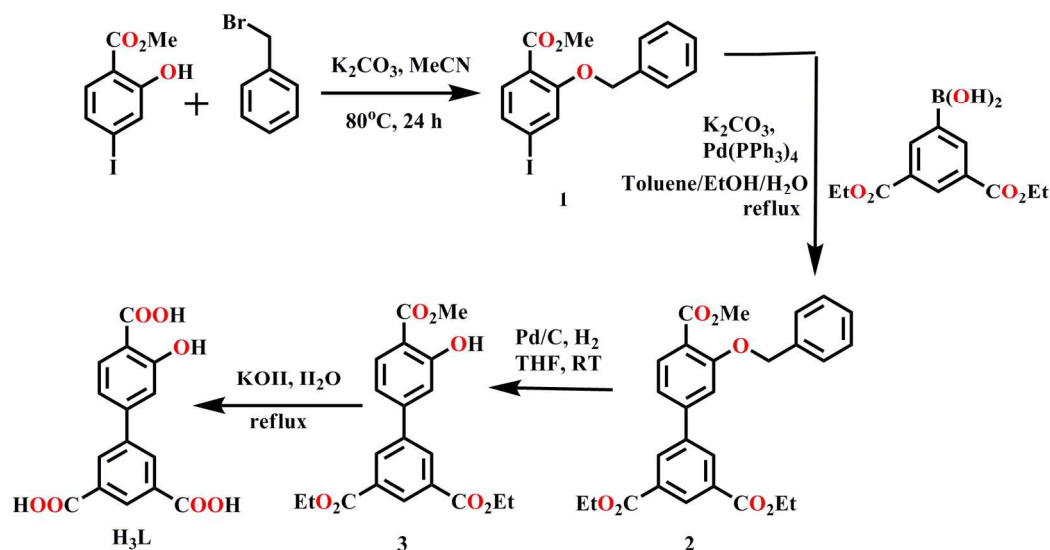
Single crystal X-ray data of **1** was collected at 100 K on a Bruker SMART APEX CCD diffractometer using graphite monochromated MoK α radiation ($\lambda = 0.71073 \text{ \AA}$) and the structure solution was completed as described earlier.³³ Several DFIX commands were used for fixing some bond distances due to inherent disorder. The disordered guest solvent molecules could not be located in the successive difference Fourier maps and hence PLATON³⁴ squeeze refinement was performed. The crystal and refinement data are collected in Table S1 (Supporting Information). Selective bond distances and angles are given in Table S2 (Supporting Information).

Luminescence measurements

All the measurements were done at room temperature. For solid state measurements, activated crystals (**1'**) were ground to powder. To investigate luminescence response in different solvents, 1 mg of the sample (**1'**) was dispersed in 5 mL of the corresponding solvent, sonicated and further diluted to equal volume (20 mL) in each case and emission intensity was measured. For all quantitative measurements, 5 mg of the powdered sample (**1'**) was dispersed in 5 mL DMF and sonicated until homogeneous suspension was obtained. This solution was then diluted to 100 mL to afford the DMF-suspended **1'** and used as the stock solution for all the measurements.

Synthesis of the Ligand

Synthesis of the linker **H₃L** could be achieved in several steps as illustrated in Scheme 1. Details of the synthetic procedure are given in the Supporting Information.



Scheme 1. Synthetic scheme for the linker **H₃L**.

Synthesis of the Complex

$\{[Tb(L)(DMA)].(DMA).(0.5H_2O)\}_n$ (**1**). This was synthesized by mixing **H₃L** (0.030 g, 0.1 mmol), $Tb(NO_3)_3 \cdot 6H_2O$ (0.09 g, 0.2 mmol), DMA (2 mL) and H_2O (1 mL) in a Teflon-lined autoclave that was heated under autogenous pressure at 100 °C for 72 h followed by slow cooling to room temperature. The resulting colorless needle-shaped crystals were isolated by filtration in ~45% yield based on **H₃L**. Anal. Calcd. for $C_{23}H_{26}N_2O_{9.5}Tb$: C, 43.07; H, 4.09; N, 4.37%. Found: C, 43.55; H, 4.27; N, 4.17%. IR (cm^{-1}): 3428(br), 2927(s), 1618(m), 1518(s), 1454(s), 1375(s), 1296(s), 1211(s), 1010(s), 774(s), 731(s) (Figure S12, Supporting Information).

RESULTS AND DISCUSSION

The PMOF **1** could be easily synthesized in single crystal form under solvothermal condition in moderate yields. The single crystal X-ray diffraction study reveals that it crystallizes in the tetragonal space group $I4_1/a$. The asymmetric unit contains one Tb(III) ion, one linker (L^{3-} , denoted as **L**) and one coordinated DMA molecule (Figure 2a).

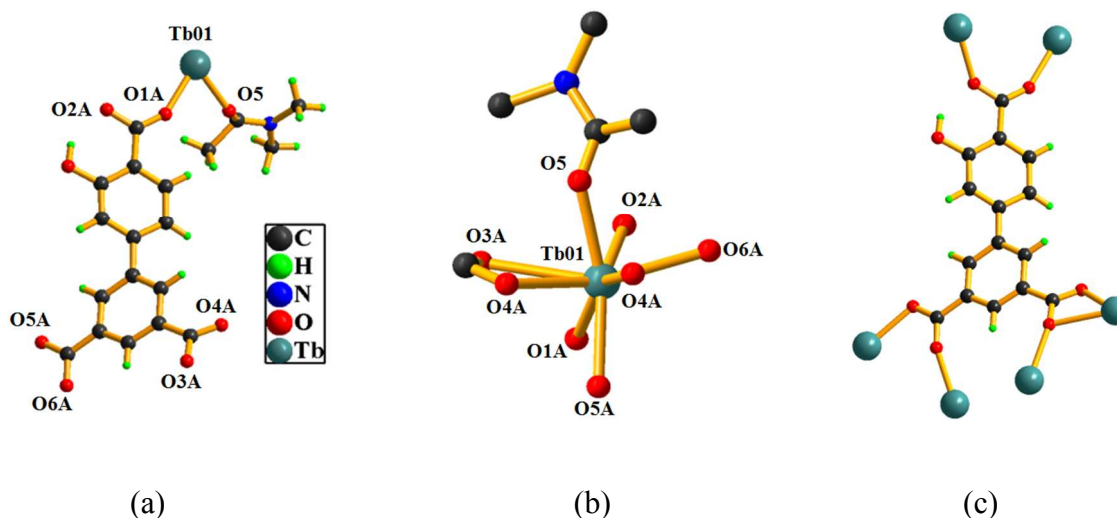


Figure 2. (a) Asymmetric unit of **1**, (b) coordination environment around Tb(III), (c) binding mode of the linker.

Each Tb^{3+} ion is coordinated to eight O atoms: one bidentate carboxylate, five monodentate carboxylate from five different *L* and one O atom from a DMA molecule (Figure 2b). The Tb-O bond distances lie in the range, 2.716(8) — 2.268(1) Å that are comparable to reported Tb-O bond distances.²⁶ The binding mode of the carboxylate towards Tb^{3+} ion is $\mu_6: \eta^1: \eta^1: \eta^1: \eta^2: \eta^1: \eta^1$ (Figure 2c). The linker is completely de-protonated during the reaction and binds Tb^{3+} ions to form a one-dimensional chain along the crystallographic *c*-axis with the nearest Tb-Tb distance being 4.330(9) Å (Figure S15a, Supporting Information). These chains are interlinked with the linker *L* along the crystallographic *a* and *b* axes (Figure S15b, c, Supporting Information) forming a three-dimensional box-like structure (Figure 3). Topological simplification shows that the framework is 6,6-*c* net forming a new network topology with Schläfli point symbol $\{4^{13}.6^2\}\{4^8.6^7\}$ (Figure S15e, Supporting Information). The solvent molecules present in the cavity are highly disordered; hence, the exact solvent composition was evaluated by the combination of TGA and elemental analysis and agreement with PLATON

1
2
3
4
5
6
7
8
9
10
11
12
13
14
15
16
17
18
19
20
21
22
23
24
25
26
27
28
29
30
31
32
33
34
35
36
37
38
39
40
41
42
43
44
45
46
47
48
49
50
51
52
53
54
55
56
57
58
59
60

calculated solvent accessible void volume (5276 Å³; 45%) of the unit cell. The channel dimensions along the crystallographic *c* direction is 15.223(3)×15.223(3) Å² and the free hydroxyl moieties of the linker are exposed in the channels along *a* and *b*-axis. Metal-bound DMA molecules are also directed towards the centre of the channels as viewed along *c*-axis.

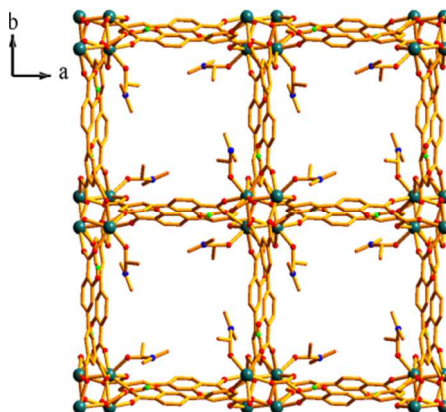


Figure 3. A perspective view of **1** along crystallographic *c*-axis (guest free, H atoms are omitted for clarity).

Thermogravimetric analysis reveals that the PMOF loses 15% of its weight (calculated 14.98%) up to 120 °C that corresponds to the loss of lattice water and DMA molecules. The coordinated DMA molecules are removed at higher temperature (up to 270 °C) showing a weight loss of 14% (calculated 13.57%). Complete decomposition of the compound is achieved beyond 400 °C (Figure S13, Supporting Information). The powder X-ray diffraction pattern of the synthesized crystals also agrees well with the simulated pattern and confirmed its phase purity. Furthermore, the VT-PXRD data indicate that the overall framework integrity of **1** is retained at temperatures at least up to 150 °C (Figure S14, Supporting Information). Single crystals of **1** were kept in EtOH for a week and then heated to 120 °C under 1 mm pressure for 10 h to obtain the activated compound **1'**. The powder pattern of **1'** matched well with the original complex **1**

(Figure S14, Supporting Information). Due to the porous character of the framework and availability of surface functionalized channels of **1**, gas adsorption studies were conducted up to a relative pressure (p/p_o) of 1.0 bar. Gas adsorption characteristics of **1'** were not significant and hence not pursued further (Figure S29, Supporting Information).

The solid-state photoluminescence spectra of the free linker (**H₃L**) and **1'** were measured under ambient conditions by exciting at 345 and 350 nm respectively (Figure 4). It is well-known that Tb^{3+} ion exhibits luminescence properties due to f-f transitions that are both spin and parity-forbidden, thereby having low intensity. However, its emission intensity can be enhanced by integrating Tb^{3+} ions with conjugated systems to cause efficient energy transfer from ligand to the Tb^{3+} -center. Thus, **1'** exhibits the characteristic enhanced luminescent emissions at λ_{max} values of 490, 544, 584, 622 nm, upon excitation at 350 nm, which can be assigned¹⁶ to $^5D_4 \rightarrow ^7F_6$, $^5D_4 \rightarrow ^7F_5$, $^5D_4 \rightarrow ^7F_4$ and $^5D_4 \rightarrow ^7F_3$ transitions, respectively. The emission arising from the free ligand ($\lambda_{max} \sim 460$ nm for **H₃L**) is not observed here. The absence of ligand-based emission in **1'** indicates efficient energy transfer from the ligand to the Tb^{3+} center (“antenna effect”) greatly enhancing the optical performance of the metal ion. The most prominent characteristic emission peak of **1'** at 544 nm makes it bright green under standard UV-lamp visible in naked eye which is an added advantage for its sensory application. Due to such luminescence property of **1'**, its emission characteristics with different electron-deficient NACs and metal ions were probed. The 3D MOF can act as a host for small guest molecules and energy transfer between them can produce a strong synergistic effect for the recognition of specific guest molecules. The complex **1'** was finely powdered and then dispersed in different selected analyte-solutions to investigate its luminescence properties.

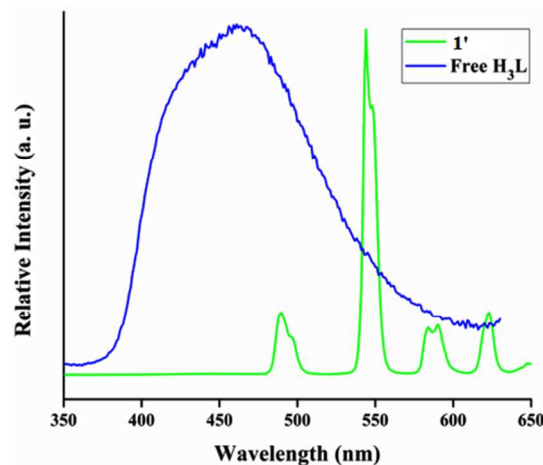
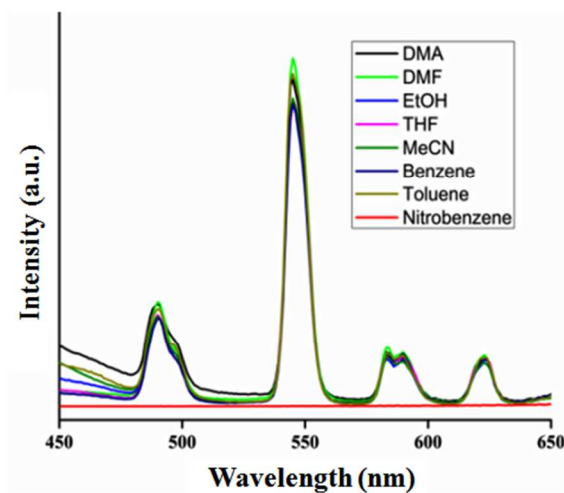
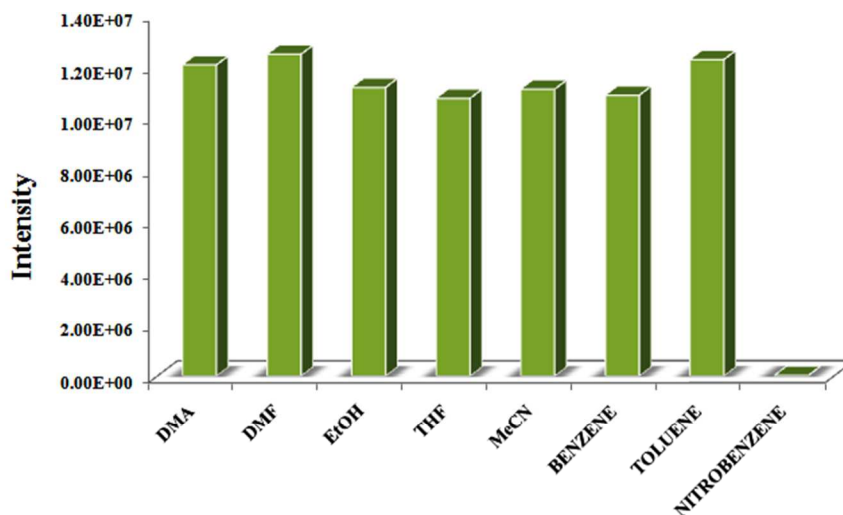


Figure 4. Solid state luminescence spectra of H_3L and that of $1'$.

Compound $1'$ was first dispersed in different commonly used organic solvents like *N,N'*-dimethylacetamide (DMA), *N,N'*-dimethylformamide (DMF), ethanol (EtOH), acetonitrile (MeCN), dioxane, tetrahydrofuran (THF), benzene and toluene as well as nitrobenzene (NB). Interestingly, it was observed that only in nitrobenzene (NB) solvent, the emission was completely quenched while with the other solvents, the variation of emission intensity was not discernible (Figure 5).



(a)



(b)



(c)

Figure 5. (a) Luminescence spectra of **1'** in different solvents, (b) bar diagram representation of the $^5D_4 \rightarrow ^7F_5$ transition at 544 nm in different solvents, (c) visual response of **1'** in various solvents monitored under UV light.

This observation provided the scope to explore the sensing ability of **1'** towards other nitroaromatic compounds. Hence, DMF solutions (1 mM) of different nitroaromatic compounds, *viz.* nitrobenzene (NB), 1,4-dinitrobenzene (1,4-DNB), 2,4-dinitrochlorobenzene (DNCB), *p*-nitrophenol (NP) and 2,4,6-trinitrophenol (TNP) were prepared. Each of these solutions (1 mL) was added to a fixed amount of DMF-suspended **1'** (0.1 mL of stock solution). Significant quenching was observed in each case (Figure 6a). The extent of quenching was calculated by using the equation $(I_0 - I)/I_0 \times 100\%$, where I_0 and I are the luminescence intensities of the stock

1
2
3
4
5
6
7
8
9
10
11
12
13
14
15
16
17
18
19
20
21
22
23
24
25
26
27
28
29
30
31
32
33
34
35
36
37
38
39
40
41
42
43
44
45
46
47
48
49
50
51
52
53
54
55
56
57
58
59
60

solution of **1'** before and after the addition of the NAC-analyte, respectively. Due to high concentration of the NAC-analytes with respect to stock solution, the emission intensity almost completely quenches in each case. To evaluate the quenching constant quantitative measurements were performed (Figure S17-S21, Supporting Information) with higher dilution of the NAC-analytes and by using the Stern-Volmer (SV) equation $(I_0/I)=K_{SV}[A]+1$, where I_0 represents the initial intensity of **1'** in absence of analyte, I is the emission intensity in presence of analyte with molar concentration $[A]$ and K_{SV} is the quenching constant (M^{-1}). The quenching efficiency by the analytes are in the following order: TNP > 4NP > DNCB > 1,4-DNB > NB (Figure 6b).

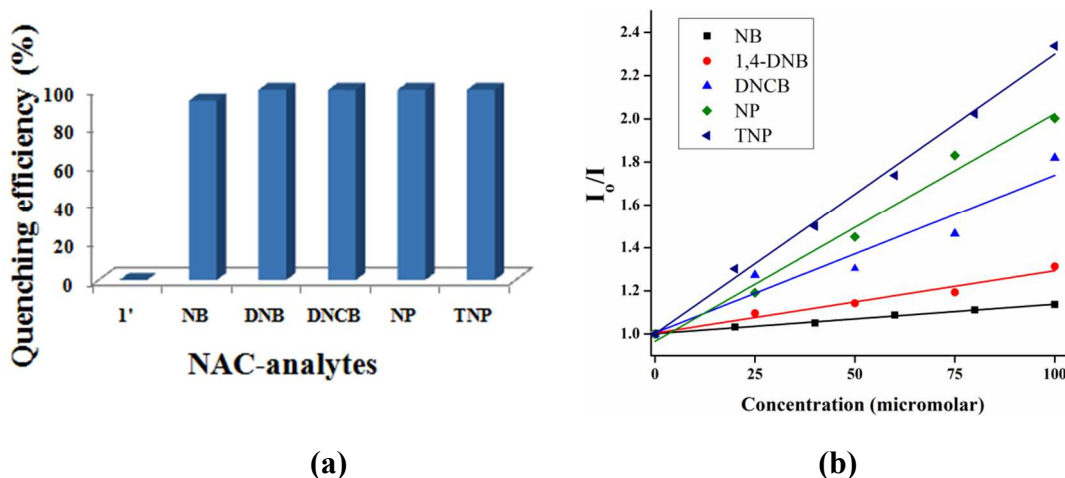


Figure 6. (a) Quenching efficiency of **1'** in presence of different nitroaromatic compounds (1mM), (b) corresponding Stern-Volmer plots of NAC-analytes.

To examine the potential of **1'** for sensing of the metal ions, DMF solution containing different metal ions (0.1 M solution of nitrate salts of Li^+ , Na^+ , K^+ , Mg^{2+} , Al^{3+} , Cr^{3+} , Mn^{2+} , Fe^{3+} , Co^{2+} , Ni^{2+} , Cu^{2+} , Zn^{2+} , Cd^{2+} , Pb^{2+} and perchlorate salt of Fe^{2+}) were added separately into a fixed amount of the stock dispersion of **1'**. The luminescence intensity quenched in presence of Fe^{3+}

ions while a moderate intensity reduction was observed upon the addition of Fe^{2+} or Cu^{2+} ions. Other metal ions do not alter the intensity to any noticeable extent as shown in Figure 7.

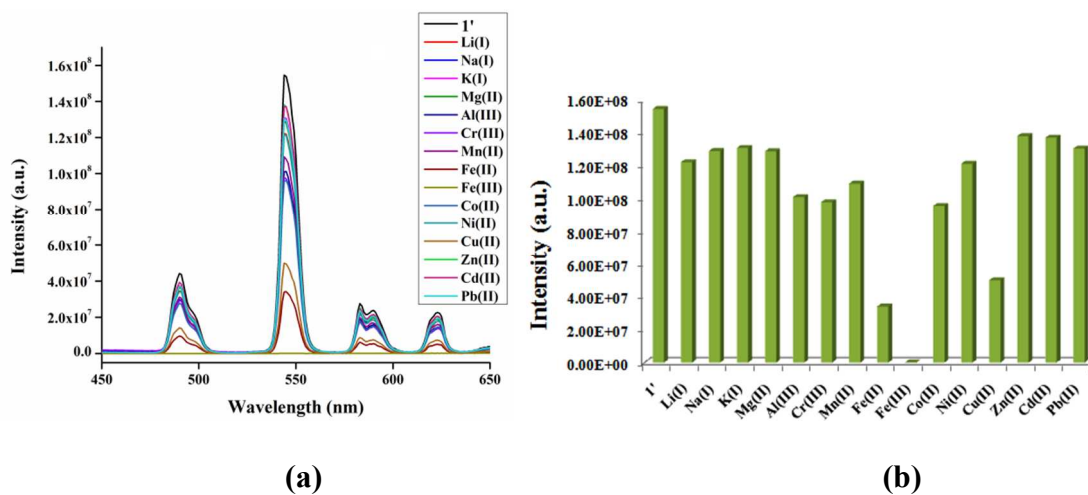


Figure 7. (a) Luminescence intensity of **1'** in presence of different metal ions (0.1 M) in DMF solution, (b) bar diagram representation of relative intensity of the same.

Interference by other metal ions with the detection of Fe^{3+} ion was investigated by competitive experiments. The results indicated that the presence of other metal ions did not make any significant change in the sensing of Fe^{3+} ions (Figure S23, Supporting Information). Quantitative emission titration experiments were also performed with Fe^{3+} ions. With the increasing concentration of Fe(III) , the emission intensity of DMF-suspended stock solution of **1'** decreased gradually (in the concentration range of 10^{-6} to 10^{-2} M) as shown in the figures 8a and S24 (Supporting Information). In the concentration range of 10^{-4} to 10^{-3} M, a good linear correlation ($R^2 = 0.99243$) between the quenching efficiency and the amount of Fe^{3+} was observed (Figure 8b).

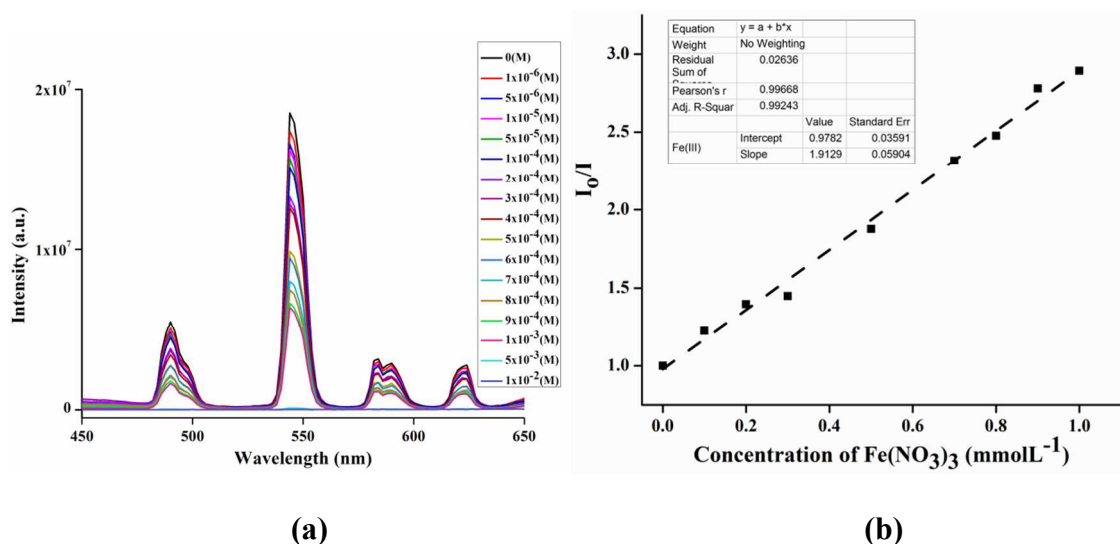


Figure 8. (a) Variation of luminescence intensity of **1'** suspension with different concentration of $\text{Fe}(\text{NO}_3)_3$, (b) corresponding Stern-Volmer plot.

For probing reversibility of the luminescence property of **1'**, it was dispersed in a DMF solution of ferric nitrate/trinitrophenol and centrifuged after one day. After washing several times with fresh DMF, the luminescence intensity of **1'** was measured. Variation of the luminescence intensity was not significant at least up to three sensing-recovery cycles in either case indicating reversibility of sensing (Figure S25, Supporting Information).

Probable mechanism of sensing

The probable mechanism for quenching of emission of **1'** in presence of the experimental analytes might be due to alternation in crystal structure, metal ion exchange, host-guest interactions or competition of absorption of excitation energy between the MOF and the analytes. The PXRD patterns of **1**, NAC-immersed **1'** and **1'** immersed in a metal salt solution (ferric nitrate, cupric nitrate) showed good agreement suggesting that the basic framework remained unaltered (Figure S22, S26, Supporting Information). An examination of the IR spectra of **1** and nitrobenzene immersed **1** showed that the peaks in **1** to be broadened and slightly red-shifted with respect to those of the pure crystals of **1** (Figure S27, Supporting Information) suggesting

1
2
3 interactions of nitrobenzene with the host framework.^{26,35} It is, therefore, presumed that the
4
5 NACs, being electron-deficient in nature, can interact with the electron-rich cavity of the
6
7 framework leading to quenching of the emission of **1'**.²⁶⁻²⁸
8
9

10 For probing the Fe³⁺ induced quenching, the possibility of transmetalation was
11 investigated. However, no transmetalation reaction in **1** was observed upon keeping crystals of **1**
12 in a 0.5 M DMF solution of ferric nitrate even after 7 d at RT as proven by the EDS experiments
13 (Table S3, Supporting Information). It is presumed, therefore, that there might exist a
14 competitive absorption of excitation energy between Fe(III) ions and **1'** which diminish the
15 essential energy requirement for the antenna effect. The overlapping of absorption band of DMF
16 solution of Fe(III) ion (strong absorption in the range of 250-500 nm) and the excitation spectra
17 of **1'** (~350 nm) also indicates this possibility (Figure. S28, Supporting Information). Similar
18 observations were found in earlier cases as well.²⁸⁻³¹
19
20
21
22
23
24
25
26
27
28
29
30
31
32
33

34 CONCLUSION

35
36 A new luminescent 3D porous Tb-MOF which contains free hydroxyl group in the
37 channels was synthesized and characterized. This framework has established another example as
38 a potential probe for sensing nitroaromatic compounds as well as cation sensing. The dispersed
39 solution of activated **1** in DMF medium reveals selective and remarkable quenching effect in
40 presence of Fe(III) ions and moderately towards Fe(II)/Cu(II) ions. Such sensing of NACs and
41 Fe(III) is reversible in nature and probably occurred through host-guest interaction and
42 competitive absorption of excitation energy respectively. Other lanthanide-MOFs with this
43 ligand have been synthesized and further studies are currently underway to examine their
44 potential applications.
45
46
47
48
49
50
51
52
53
54
55
56
57
58
59
60

ASSOCIATED CONTENT

Supporting Information.

The Supporting Information is available free of charge on the ACS Publications website at DOI:

Additional experiments and structural figures, X-ray crystallographic data, TGA, and PXRD patterns of **1** (PDF).

Accession Codes

CCDC 1485393 contains the supplementary crystallographic data for this paper. These data can be obtained free of charge via www.ccdc.cam.ac.uk/data_request/cif, or by emailing data_request@ccdc.cam.ac.uk, or by contacting The Cambridge Crystallographic Data Centre, 12 Union Road, Cambridge CB2 1EZ, UK; fax: +44 1223 336033.

AUTHOR INFORMATION

Corresponding Author

*E-mail: pkb@iitk.ac.in.

Notes

The authors declare no competing financial interest.

ACKNOWLEDGEMENTS

We gratefully acknowledge the financial support received from the Department of Science and Technology, New Delhi, India (to PKB) and SRF from the CSIR to S.P. We also acknowledge Dr. Subhadip Neogi for gas adsorption measurements.

REFERENCES

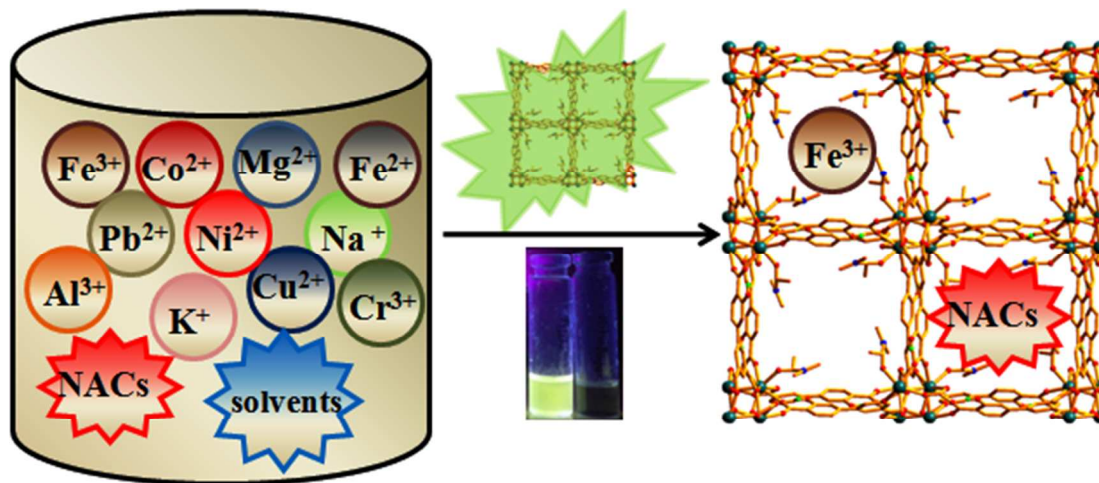
- (1) Rosi, N. L.; Eckert, J.; Eddaoudi, M.; Kim, D. T. J.; O'Keefe, M.; Yaghi, O. M. *Science* **2003**, *300*, 1127-1129.
- (2) Biradha, K.; Ramanan, A.; Vittal, J. J. *Cryst. Growth Des.* **2009**, *9*, 2969-2970.
- (3) Santra, A.; Senkovska, I.; Kaskel, S.; Bharadwaj, P. K. *Inorg. Chem.* **2013**, *52*, 7358-7366.
- (4) He, C.; Lu, K.; Liu, D.; Lin, W. *J. Am. Chem. Soc.* **2014**, *136*, 5181-5184.
- (5) Aijaz, A.; Akita, T.; Tsumori, N.; Xu, Q. *J. Am. Chem. Soc.* **2013**, *135*, 16356-16359.
- (6) Mukherjee, G.; Biradha, K. *Cryst. Growth Des.* **2014**, *14*, 3696-3699.
- (7) Nagarkar, S. S.; Unni, S. M.; Sharma, A.; Kurungot, S.; Ghosh, S. K. *Angew. Chem. Int. Ed.* **2014**, *53*, 2638-2642.
- (8) Hu, Z.; Deiberta, B. J.; Li, J. *Chem. Soc. Rev.* **2014**, *43*, 5815-5840.
- (9) Cui, Y.; Yue, Y.; Qian, G.; Chen, B. *Chem. Rev.* **2012**, *112*, 1126-1162.
- (10) Kreno, L. E.; Leong, K.; Farha, O. K.; Allendorf, M.; Van Duyne, R. P.; Hupp, J. T. *Chem. Rev.* **2012**, *112*, 1105-1125.
- (11) Nagarkar, S. S.; Desai, A. V.; Ghosh, S. K. *CrystEngComm*, **2016**, *18*, 2994-3007.
- (12) Germain, M. E.; Knapp, M. J. *Chem. Soc. Rev.* **2009**, *38*, 2543 - 2555.
- (13) Wollin, K. M.; Dieter, H. H. *Arch. Environ. Contam. Toxicol.* **2005**, *49*, 18-26.
- (14) Zhang, L.; Kang, Z.; Xin, X.; Sun, D. *CrystEngComm*. **2016**, *18*, 193-206.
- (15) Pal, S.; Chatterjee, N.; Bharadwaj, P. K. *RSC Adv.* **2014**, *4*, 26585-26620.
- (16) Cui, Y.; Chen, B.; Qian, G. *Coord. Chem. Rev.* **2014**, *273-274*, 76-86.
- (17) Bünzli, J. -C. G.; Piguet, C. *Chem. Soc. Rev.* **2005**, *34*, 1048-1077.
- (18) Gole, B.; Bar, A. K.; Mukherjee, P. S. *Chem. Eur. J.* **2014**, *20*, 2276 - 2291.
- (19) Gole, B.; Bar, A. K.; Mukherjee, P. S. *Chem. Eur. J.* **2014**, *20*, 13321 - 13336.
- (20) Shanmugaraju, S.; Mukherjee, P. S. *Chem. Eur. J.* **2015**, *21*, 6656 - 6666.
- (21) Lan, A.; Li, K.; Wu, H.; Olson, D. H.; Emge, T. J.; Ki, W.; Hong, M.; Li, J. *Angew. Chem. Int. Ed.* **2009**, *48*, 2334 - 2338.
- (22) Pramanik, S.; Hu, Z.; Zhang, X.; Zheng, C.; Kelly, S.; Li, J. *Chem. Eur. J.* **2013**, *19*, 15964 - 15971.

- 1
2
3
4
5 (23) Nagarkar, S. S.; Joarder, B.; Chaudhari, A. K.; Mukherjee, S.; Ghosh, S. K. *Angew. Chem.*
6 *Int. Ed.* **2013**, *52*, 2881-2885.
7
8 (24) Joarder, B.; Desai, A. V.; Samanta, P.; Mukherjee, S.; Ghosh, S. K. *Chem. Eur. J.* **2015**, *21*,
9 965 – 969.
10
11 (25) Wang, W.; Yang, J.; Wang, R.; Zhang, L.; Yu, J.; Sun, D. *Cryst. Growth Des.* **2015**, *15*,
12 2589-2592.
13
14 (26) Wang, J.; Sun, W.; Chang, S.; Liu, H.; Zhang, G.; Wang, Y.; Liu, Z. *RSC Adv.*, **2015**, *5*,
15 48574–48579.
16
17 (27) Sun, W.; Wang, J.; Liu, H.; Chang, S.; Qin, X.; Liu, Z. *Materials Letters*, **2014**, *126*, 189–
18 192.
19
20 (28) Zhao, X.-L.; Tian, D.; Gao, Q.; Sun, H.-W.; Xu, J.; Bu, X.-H. *Dalton Trans.*, **2016**, *45*,
21 1040-1046.
22
23 (29) Cao, L.-H.; Shi, F.; Zhang, W.-M.; Zang, S.-Q.; Mak, T. C. W. *Chem. Eur. J.* **2015**, *21*,
24 15705 – 15712.
25
26 (30) Liang, Y.-T.; Yang, G.-P.; Liu, B.; Yan, Y.-T.; Xi, Z.-P.; Wang, Y.-Y. *Dalton Trans.*, **2015**,
27 44, 13325–13330.
28
29 (31) Wen, R.-M.; Han, S.-D.; Ren, G.-J.; Chang, Z.; Li Y.-W. Bu, X.-H. *Dalton Trans.*, **2015**,
30 44, 10914-10917.
31
32 (32) Sun, W.; Wang, J.; Zhang, G.; Liu, Z. *RSC Adv.*, **2014**, *4*, 55252–55255.
33
34 (33) Pal, T. K.; Katoch, R.; Garg, A.; Bharadwaj, P. K. *Cryst. Growth Des.* **2015**, *15*, 4526-4535.
35
36 (34) Spek, A. L., PLATON; The University of Utrecht: Utrecht, The Netherlands, **1999**.
37
38 (35) Di, L.; Zhang, J. -J.; Liu, S. -Q.; Ni, J.; Zhou, H.; Sun, Y. -J. *Cryst. Growth Des.* **2016**, *16*,
39 4539-4546.
40
41
42
43
44
45
46
47
48
49
50
51
52
53
54
55
56
57
58
59
60

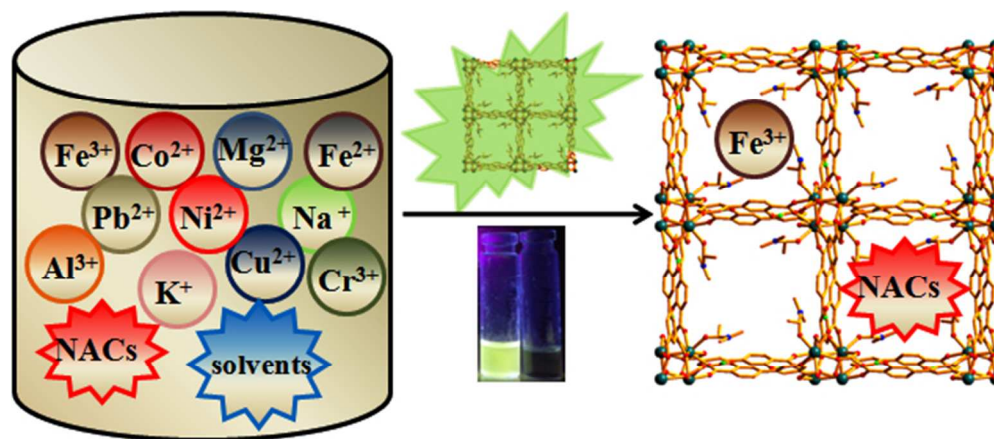
For Table of Contents Use Only

A Luminescent Terbium MOF Containing Hydroxyl Groups Exhibits Selective Sensing of Nitroaromatic Compounds and Fe(III) Ions

Sanchari Pal and Parimal K. Bharadwaj*



A new 3D porous Tb(III)-ion based PMOF has been synthesized which selectively sense nitroaromatic compounds and Fe(III) ions in DMF suspension by fluorescence quenching mechanism.



A new 3D porous Tb(III)-ion based PMOF has been synthesized which selectively sense nitroaromatic compounds and Fe(III) ions in DMF suspension by fluorescence quenching mechanism.

169x75mm (96 x 96 DPI)